



Contents lists available at ScienceDirect

Journal of King Saud University – Science

journal homepage: www.sciencedirect.com



## Original article

## Electroacupuncture ameliorates endotoxin-induced acute lung injury in rabbits by regulating heme oxygenase-1 expression to improve mitochondrial dynamics

Yuan Zhang<sup>a,1</sup>, Wei-wei Zhang<sup>b,1</sup>, Jia Shi<sup>a,1</sup>, Tian-yu Yu<sup>c</sup>, Jian-bo Yu<sup>a,\*</sup>, Shi-han Du<sup>c</sup>, Si-meng He<sup>d</sup>, Kai Song<sup>a</sup><sup>a</sup> Department of Anesthesiology, Tianjin Nankai Hospital, Tianjin 300100, China<sup>b</sup> Department of Anesthesiology, Tianjin Medical University Nankai Hospital, Tianjin 300100, China<sup>c</sup> Tianjin Medical University, Tianjin 300070, China<sup>d</sup> Department of Anesthesiology, Nankai University Nankai Hospital, Tianjin, 300100, China

## ARTICLE INFO

## Article history:

Received 30 October 2019

Revised 18 November 2019

Accepted 21 November 2019

Available online 2 December 2019

## Keywords:

Heme oxygenase-1

Electroacupuncture

Lung injury

Mitochondrial dynamics

## ABSTRACT

**Background:** Electroacupuncture (EA) mitigates endotoxin-induced acute lung injury (ALI) during bacterial sepsis, but the mechanisms are unclear. This study aimed to investigate the potential mechanisms of EA improving endotoxin-induced ALI.**Methods:** Endotoxin-induced ALI was established by lipopolysaccharide (LPS) administration. Electroacupuncture was started 5 days before LPS administration and non-acupoint EA (punctured at non-acupoints with shallow insertion and no electrical stimulation) was used as the control treatment. In addition, hemin was applied to active HO-1 and ZnPP to suppress HO-1. Briefly, 70 rabbits were divided into seven treatment groups: untreated control (C), LPS, LPS + EA, LPS + non-acupoint EA, LPS + EA + hemin, LPS + EA + ZnPP, and LPS + EA + ZnPP + hemin. Lung samples were collected at 6 h after LPS administration for analysis of tissue injury (edema, inflammation, hemorrhage, necrosis), oxidative stress, mitochondrial membrane potential (MMP), respiratory control ratio (RCR), ATP production, and changes in expression of mitochondrial fusion and fission markers.**Results:** Electroacupuncture alleviated LPS-induced lung injury and mitochondria dysfunction as indicated by decreasing wet/dry tissue weight ratio, lung injury score, ROS production, and suppressing expression of mitochondrial fission proteins. Furthermore, EA also increased ATP content, mitochondrial membrane potential, respiratory control ratio, and expressions of mitochondrial fusion proteins (LPS + EA group vs. LPS group). These effects of EA were further enhanced by pretreatment with hemin (LPS + EA + hemin group) but suppressed by Znpp-IX (LPS + EA + ZnPP and LPS + EA + ZnPP + hemin groups). **Conclusions:** Electroacupuncture protects against endotoxin-induced ALI by upregulating heme oxygenase-1 expression, thereby preserving the balance between mitochondrial fusion and fission.© 2019 Published by Elsevier B.V. on behalf of King Saud University. This is an open access article under the CC BY-NC-ND license (<http://creativecommons.org/licenses/by-nc-nd/4.0/>).**Abbreviations:** EA, electroacupuncture; ALI, acute lung injury; LPS, lipopolysaccharide; HO-1, heme oxygenase-1; MMP, mitochondrial membrane potential; RCR, respiratory control ratio; ROS, reactive oxygen species; DCFH-DA, 2,7-dichlorofluorescein diacetate; H&E, hematoxylin and eosin; SDS-PAGE, tris-glycine-SDS polyacrylamide gel; SD, standard deviation (SD); ANOVA, one-way analysis of variance; LSD, least significant difference; Mfn1, mitofusin 1; Mfn2, mitofusin 2; OPA1, optic atrophy protein 1; Drp1, dynamic related protein 1.

\* Corresponding author at: Department of Anesthesiology, Tianjin Nankai Hospital, No. 6 Changjiang Road, Nankai District, Tianjin 300100, China.

E-mail address: [yujianbo11@126.com](mailto:yujianbo11@126.com) (J.-b. Yu).<sup>1</sup> These authors are contributed equally for this manuscript and they are co-first authors for this research.

Peer review under responsibility of King Saud University.

## 1. Introduction

Endotoxin-induced acute lung injury (ALI) is a common complication of bacterial sepsis that markedly increases mortality (Schlosser et al., 2018). Indeed, despite therapeutic advances aimed at ameliorating endotoxin-induced ALI, mortality is still high, reaching 35.1% to 46.1% (Rubinfeld et al., 2005). Thus, safer and more effective therapeutic measures are urgently required (Shafeeq and Lat, 2012). A number of studies have shown that acupuncture is effective against multiple diseases including stress-associated urinary incontinence, postoperative intra-abdominal adhesions, asthma, and pulmonary diseases (Liu et al., 2017; Du et al., 2015; Nurwati et al., 2019; Suzuki et al., 2018; Pan et al., 2010). Our previous clinical trial demonstrated that EA can improve oxygenation index and decrease APACHE-II score of



Production and hosting by Elsevier

<https://doi.org/10.1016/j.jksus.2019.11.029>

1018-3647/© 2019 Published by Elsevier B.V. on behalf of King Saud University.

This is an open access article under the CC BY-NC-ND license (<http://creativecommons.org/licenses/by-nc-nd/4.0/>).

patients with sepsis-induced lung injury, but the mechanism is still unknown (Li et al., 2017). Many studies on the therapeutic mechanisms of acupuncture in sepsis have focused on mitigation of oxidative stress (Han et al., 2017; Chen et al., 2016a), which is consistent with our previous studies that EA could suppress the reactive oxygen species (ROS) accumulation in endotoxin-induced ALI (Yu et al., 2013; Zhang et al., 2014).

Mitochondria are the primary targets of oxidative damage. Mitochondrial function under oxidative stress is maintained by the balance of fusion and fission cycles (Youle and van der Bliek, 2012). Proper regulation of mitochondrial fusion/fission balance is vital for protection from oxidative damage during endotoxin-induced ALI (Zhang et al., 2019a; Dong et al., 2018). However, the exact molecular mechanisms controlling mitochondrial dynamics in endotoxin-induced lung injury are still poorly understood. Our previous studies found that EA attenuated endotoxin-induced ALI by upregulating heme oxygenase 1 (HO-1) (Yu et al., 2013; Zhang et al., 2014) and some reports indicated that HO-1 is one of modulators of the mitochondrial fusion/fission balance (Yu et al., 2016). However, the effect of EA on mitochondrial fusion/fission balance has not been clearly discussed. This study aimed to clarify the influence of EA on mitochondrial fusion/fission balance and the role of HO-1 in lung protection from oxidative injury during endotoxin-induced ALI. The central hypothesis is described schematically in Fig. 1.

**2. Material and methods**

*2.1. Materials*

Antibodies against HO-1 (D51619) and Drp1 (D61517) were purchased from Boote Biotechnology (Wuhan, China). Antibodies against Mfn1 (AE082042), Mfn2 (AF01270996B) and OPA1 (AD090106) were purchased from Bioss Biotechnology (Beijing, China). The 2,7-dichlorofluorescein diacetate (DCFH-DA) and ATP enzyme test kits were acquired from Nanjing Jiancheng Bioengineering Institute (Nanjing, China). All other chemicals including

LPS (L1245), Znpp-IX (MKBV8659V), and hemin (BCBM3691V), were obtained from Sigma (St. Louis, MO, USA).

*2.2. Animals and grouping*

Two-month-old male New Zealand white rabbits (1.52.0 kg) were purchased from the Institute of Radiation Medicine of the Chinese Academy of Medical Sciences. Rabbits were maintained individually under a 12 h light/dark cycle, 30% to 70% humidity, and 23±2°C with ad libitum access to standard rabbit chow and distilled water. Animals were acclimated for three days prior to experiments.

Rabbits were divided into seven treatment groups with ten animals per group: control (C), LPS (LPS injection as a model of endotoxin-induced ALI), LPS + EA (EA pretreatment plus endotoxin-induced ALI), LPS + non-acupoint EA (non-acupoint EA pretreatment and endotoxin-induced ALI), LPS + EA + hemin, LPS + EA + ZnPP, and LPS + EA + ZnPP + hemin.

*2.3. Endotoxin-induced ALI model*

The rabbits were weighed and injected with 2% pentobarbital sodium (60 mg/kg) for anesthesia. Lipopolysaccharide (5 mg/kg, Sigma, USA) reconstituted in 1 mL sterile sodium chloride, 0.9%, was then injected to model endotoxin-induced ALI. Some rabbits were pretreated intravenously with 100 mg/kg hemin (dissolved in 0.1 mmol/L sodium hydroxide) or 10 mol/kg Znpp-IX (dissolved in 1 mL sodium bicarbonate) 1 h before LPS injection (Yu et al., 2013; Privitera et al., 2007). All rabbits were euthanized by exsanguination from the jugular vein under anesthesia at 6 h after LPS stimulation. Lung tissues were collected for further studies.

*2.4. Electroacupuncture procedures*

Electroacupuncture was initiated 5 days before LPS treatment (ALI modeling) in the indicated groups (LPS + EA, LPS + EA + hemin, LPS + EA + ZnPP, and LPS + EA + ZnPP + hemin). Two pairs of stainless steel acupuncture needles were inserted bilaterally into the

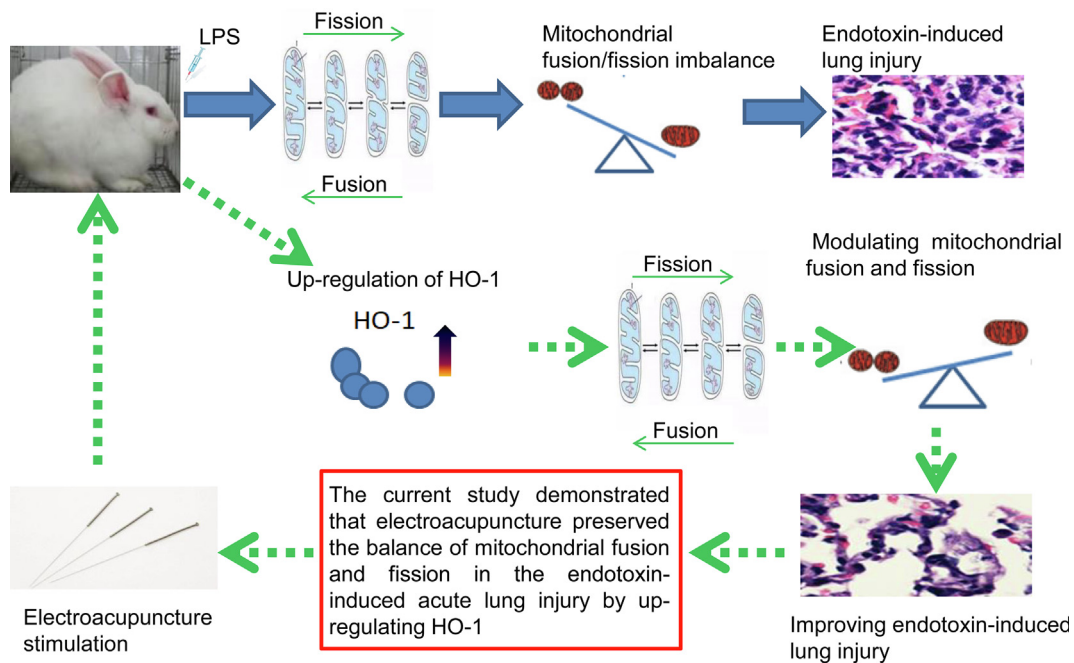


**Fig. 1.** The outline of experiment design.

rabbit equivalent of the ST36 acupoint and the BL13 acupoint according to the previous research (Yu et al., 2013). Electroacupuncture stimulation was delivered by Hans acupoint nerve stimulator (LH-202H, Neuroscience Research Institute, Beijing, China) by disperse-dense wave at 2/100 Hz for 30 min every day for five consecutive days before LPS injection (Ferreira et al., 2009). The final EA administration was delivered on the day of LPS treatment (Wang et al., 2009). Non-acupoint EA at non-acupoints with shallow insertion and no electrical stimulation was used as the control treatment for EA (Chen et al., 2016b; Chen et al., 2017). An experienced acupuncturist identified the acupoints and non-acupoints.

### 2.5. Lung histopathology

Lung tissue was dissected and stored in 70% ethanol. Sections were stained with hematoxylin and eosin (H&E) dye. Lung histopathology was assessed from at least 3 rabbits per treatment group by a pathologist who was blinded to treatment history. Digital photos of lung tissues were imaged using a Leica microscope (DM IRB, Leica Microsystems, Wetzlar, Germany) and analyzed by Image-Pro Plus software (Media Cybernetics, Rockville, MD, USA) (Hull et al., 2016). The severity degree of lung injury was assessed according to the occurrence of edema, inflammation and hemorrhage of alveolar and interstitial, atelectasis and necrosis. Each pathology was classified as range from grade 0 to 4, according to the division principle as no injury defined as 0, 25% injury (the lesion area/the entire area in lung tissue) as 1, 50% injury as 2, 75% injury as 3, 100% injury as 4. The total lung lesion score was calculated as the sum of these scores (Zhang et al., 2019b).

### 2.6. Lung wet/dry weight ratio

The left lung was carefully dissected and immediately weighted as W(wet). Then, the lung was dried at 70°C and weighted again as W(dry). The relative water content (W/D value) = W(wet)/W(dry).

### 2.7. ROS production

Reactive oxygen species accumulation, an index of oxidative stress, was measured fluorometrically using the fluorescent probe DCFH-DA. DCFH-DA is cleaved by intracellular esterase to yield nonfluorescent DCFH, which is oxidized by peroxides to highly fluorescent DCF. Briefly, cells were plated in 96-well plates and cultured to almost 80% confluence. Cell suspensions were loaded with 10<sup>6</sup> mol/L DCFH-DA for 30 min at 37°C and DCF fluorescence monitored by a Chameleon microplate reader (Hidex, Turku, Finland) at 480/530 nm (Ex/Em). The results are reported as change in fluorescence relative to baseline (F/F) (Yu et al., 2016).

### 2.8. ATP content

ATP content was determined by a commercial ATP enzyme test kit and normalized to protein using a quantitative protein assay.

### 2.9. Mitochondrial membrane potential

Freshly excised lung tissues were washed, minced and homogenized in buffer (10<sup>2</sup> mol/L HEPES, 1 mol/L mannitol, 3.5 × 10<sup>1</sup> mol/L sucrose, 5 × 10<sup>3</sup> mol/L EGTA, pH = 7.5) supplemented with bovine serum albumin at 4°C. The homogenate was centrifuged at 600g for 5 min at 4°C. The supernatants were transferred and centrifuged at 11,000g for 10 min at 4°C. Pellets containing mitochondria were suspended in a storage buffer (10<sup>2</sup> mol/L HEPES, 1.25 mol/L sucrose, 5 × 10<sup>3</sup> mol/L ATP, 4 × 10<sup>4</sup> mol/L ADP, 2.5 × 10<sup>2</sup> mol/L sodium succinate, 10<sup>2</sup> mol/L K<sub>2</sub>HPO<sub>4</sub>,

5 × 10<sup>3</sup> mol/L DTT, pH = 7.5). Mitochondrial membrane potential was assessed immediately from freshly isolated mitochondria using JC-1 as previously described (Qin et al., 2012).

### 2.10. Respiratory control ratio (RCR)

Lung tissue in the lesioned area was homogenized and the mitochondria were isolated by centrifuging homogenate twice at 12,000g for 10 min at 4°C. 1 mg mitochondria were resuspended by 1.5 mL of reaction medium (7 × 10<sup>2</sup> mol/L sucrose, 1 × 10<sup>3</sup> mol/L EDTA, 2.25 × 10<sup>1</sup> mol/L mannitol, 10<sup>2</sup> mol/L potassium phosphate, 0.1% BCA, pH = 7.4, 25°C) to acquire 2.4 × 10<sup>1</sup> mol/L mitochondrial solution. Then, 4 × 10<sup>3</sup> mol/L substrate disodium succinate was blended with the same volume of mitochondrial solution and incubated for 2 min. The respiratory oxygen quotient IV (R4) was measured using Clarks oxygen electrode method. Then, the respiratory oxygen quotient III (R3) was measured after 20 L, 5 × 10<sup>2</sup> mol/L adenosine diphosphate being added. The mitochondrial RCR = R3/R4 (Long et al., 2019).

### 2.11. Real-time PCR

Tissue RNA was extracted from rabbit lung tissues by a high-purity RNA kit (Roche, Germany) and quantified by absorbance at 260 nm using a spectrophotometer as described (Zhang et al., 2014). Then, 5 L total RNA was reversed transcribed to produce complementary DNA and the cDNA was reverse transcribed by PCR using SYBR Green Master Mix on an ABI Prism 7000 sequence detector system (Applied Biosystems, Foster City, USA). Pre-degeneration of the PCR mix was performed at 95°C for 10 min, followed by 40 thermal cycles of denaturing for 30 s at 95°C, annealing for 5 s at 95°C, and extension for 34 s at 60°C. All primers are listed in Table 1. -actin was used as an internal control to normalize all PCR products. Target gene expression was quantified using the comparative threshold cycle C<sub>T</sub> method.

### 2.12. Western blot analysis

For total proteins extraction, tissue samples were homogenized in lysis buffer and then centrifuged at 10,000g for 15 min at 4°C. 50 µg protein sample was subjected to 12% SDS-PAGE and then transferred to PVDF membranes. The membranes were carefully washed by 1 × Tris-buffered saline and then incubated with primary antibodies against HO-1 (1:1000, Booute Biotechnology), Mfn1 (1:1000, Bioss Biotechnology), Mfn2 (1:1500, Bioss Biotechnology), OPA1 (1:1000; Bioss Biotechnology), and Drp1 (1:1000; Booute Biotechnology) overnight at 4°C. -actin (1:800, Bioss Biotechnol-

**Table 1**  
PCR primer sequences.

Gene	Sequence	Size (bp)	
HO-1	Forward	CCTGGAGGAGGAGATTG	147
	Reverse	GGCGTGTAGGGGATGGT	
Mfn1	Forward	TTCTGAATAATCGTTGG	131
	Reverse	CTGTGCTTCTAATGGAT	
Mfn2	Forward	AAGTGGCTTTTTTGGC	175
	Reverse	CTCCTCTCTCCTCGGA	
OPA1	Forward	GGAAATTGATGAGTATA	187
	Reverse	TAACAAGAGAAGTAGGT	
Drp1	Forward	TACTGTGGAGTGTGTTCA	202
	Reverse	CACCTCTCTTTGTTTTT	
-actin	Forward	CAGGGCTGCCTTCTCTTGTG	186
	Reverse	TCTCGCTCTGGAAGATGGT	

Note: All sequences are in the 5 to 3 orientation.

ogy) was used as the gel loading control. Blots were clearly washed by TBS-0.05% Tween 20 and incubated by secondary antibody at 37°C for 2 h (1:3000; CWBIO, Beijing, China). The protein bands were visualized as previously described and quantified by densitometry (Zhang et al., 2014). The protein intensities of HO-1, Mfn1, Mfn2, OPA1, and Drp1 were normalized to  $\beta$ -actin intensity using the optical density ratio.

2.13. Electron microscopy

For electron microscopy, tissue was fixed in 0.1 mol/L sodium cacodylate buffer (pH = 7.3) containing 3% glutaraldehyde and 2% paraformaldehyde. Morphometric analyses were performed using NIH ImageJ (version 1.43) (Bueno et al., 2015).

2.14. Statistical analysis

Continuous variables are represented as mean  $\pm$  standard deviation (SD). Differences among group means were evaluated by one-way analysis of variance (ANOVA) and post hoc least significant difference (LSD) tests for pair-wise comparisons. A  $p < 0.05$  (two-tailed) was considered statistically significant. The Statistical Analysis System (v 9.2, SAS Institute, Inc., Cary, NC, USA) was applied to perform the statistical analysis.

2.15. Ethics approval

All experiments were approved by the Animal Ethical and Welfare Committee of Institute of Radiation Medicine of Chinese

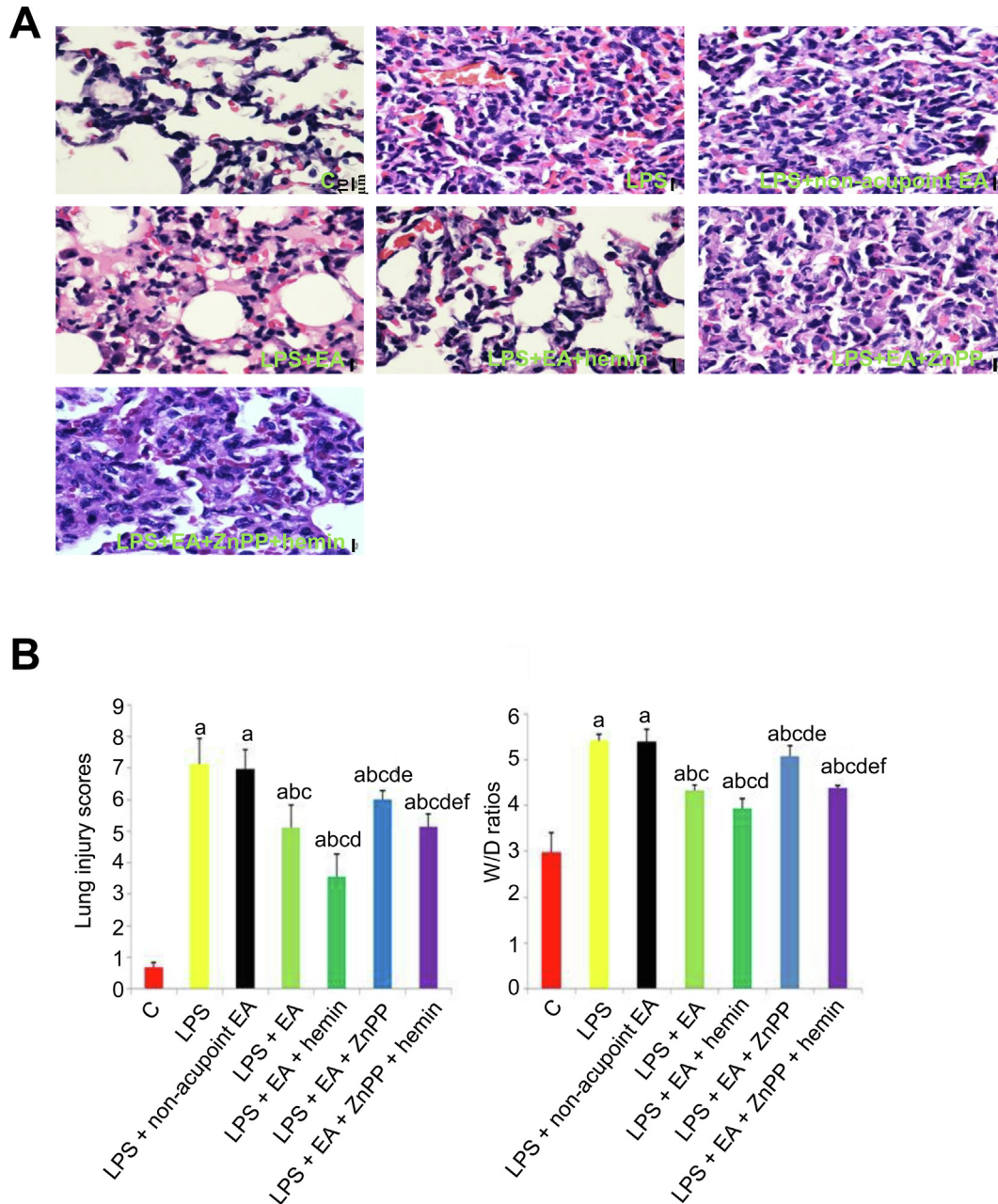


**Fig. 2.** Electroacupuncture and HO-1 upregulation mitigated LPS-induced ALI. (A) Representative images of H&E-stained lung tissue slices from the control group, LPS group, LPS + non-acupoint EA group, LPS + EA group, LPS + EA + hemin group, LPS + EA + ZnPP group and LPS + EA + ZnPP + hemin group. 400  $\times$  magnification, scale bar = 10  $\mu$ m. (B) Electroacupuncture and HO-1 upregulation suppressed quantitative metrics of lung injury. Lung injury scores and W/D ratios were expressed as mean  $\pm$  SD ( $n = 10$ ).  $ap < 0.05$  vs. Control group;  $bp < 0.05$  vs. LPS group;  $cp < 0.05$  vs. LPS + non-acupoint EA group;  $dp < 0.05$  vs. LPS + EA group;  $ep < 0.05$  vs. LPS + EA + hemin group;  $f p < 0.05$  vs. LPS + EA + ZnPP group.

Academy of Medical Sciences (No. DWLI-20160626) and performed according to the National Institutes of Health Guidelines for the Care and Use of Laboratory Animals.

### 3. Results

#### 3.1. Effects of EA and HO-1 expression on LPS-induced lung histopathology, lung injury score, and W/D ratio

The procedures of this study were as follows: EA was delivered for 30 min every day for five consecutive days (days 15) before LPS treatment. LPS (5 mg/kg) was injected as an experimental model of endotoxin-induced ALI. Some rabbits were pretreated intravenously with 100 mg/kg hemin or 10 mol/kg Znpp-IX 1 h before LPS injection. Rabbits were euthanized and tissue samples were collected 6 h after LPS injection.

Photomicrographs of excised lung tissue indicated that LPS induced thickening of the alveolar wall, infiltration of inflammatory cells into alveolar spaces, hemorrhage, and formation of hyaline membrane (Fig. 2A). All of these pathological signs of ALI were reduced by 5 days of EA pretreatment. Additional pretreatment with the HO-1 inducer hemin augmented the effects of EA, while pretreatment with the HO-1 inhibitor ZnPP-IX weakened the protective effects of EA and EA + hemin against LPS-induced ALI. In contrast to EA, non-acupoint stimulation had no effect on ALI (Fig. 2B). In summary, W/D ratio and lung injury score were increased significantly in all LPS-treated groups compared to

untreated controls ( $p < 0.05$ ), but were reduced in the LPS + EA group compared to the LPS group and the LPS + non-acupoint EA group (both  $p < 0.05$ ). Lung lesion score and W/D value were further reduced in the LPS + EA + hemin group but elevated in LPS + EA + ZnPP group compared to the LPS + EA group (both  $p < 0.05$ ). Lung lesion score and W/D value were also higher in the LPS + EA + ZnPP and LPS + EA + ZnPP + hemin groups compared to the LPS + EA + hemin group (all  $p < 0.05$ ). Finally, lung lesion score and W/D value were significantly lower in the LPS + EA + ZnPP + hemin group compared to the LPS + EA + ZnPP group ( $p < 0.05$ ). These findings strongly suggest that EA reduces LPS-evoked ALI via HO-1 upregulation.

#### 3.2. Effects of EA and HO-1 expression on LPS-induced mitochondrial dysfunction and oxidative stress

Compared to group C, ATP content, MMP, and RCR were significantly reduced while ROS production was significantly elevated in all LPS treatment groups ( $p < 0.05$ ) (Fig. 3). However, ATP content, MMP, and RCR were higher and ROS production was lower in the LPS + EA group compared to the LPS group and LPS + non-acupoint EA group ( $p < 0.05$ ), which indicated that EA improved the LPS-induced ALI at least in this four factors. Otherwise, hemin could further ameliorated ATP content, MMP, RCR and ROS production, compared LPS + EA + hemin with LPS + EA, and ZnPP didn't decrease the ROS production in LPS + EA + ZnPP group, compared with LPS + EA group. Consistent with ALI analyses, these findings

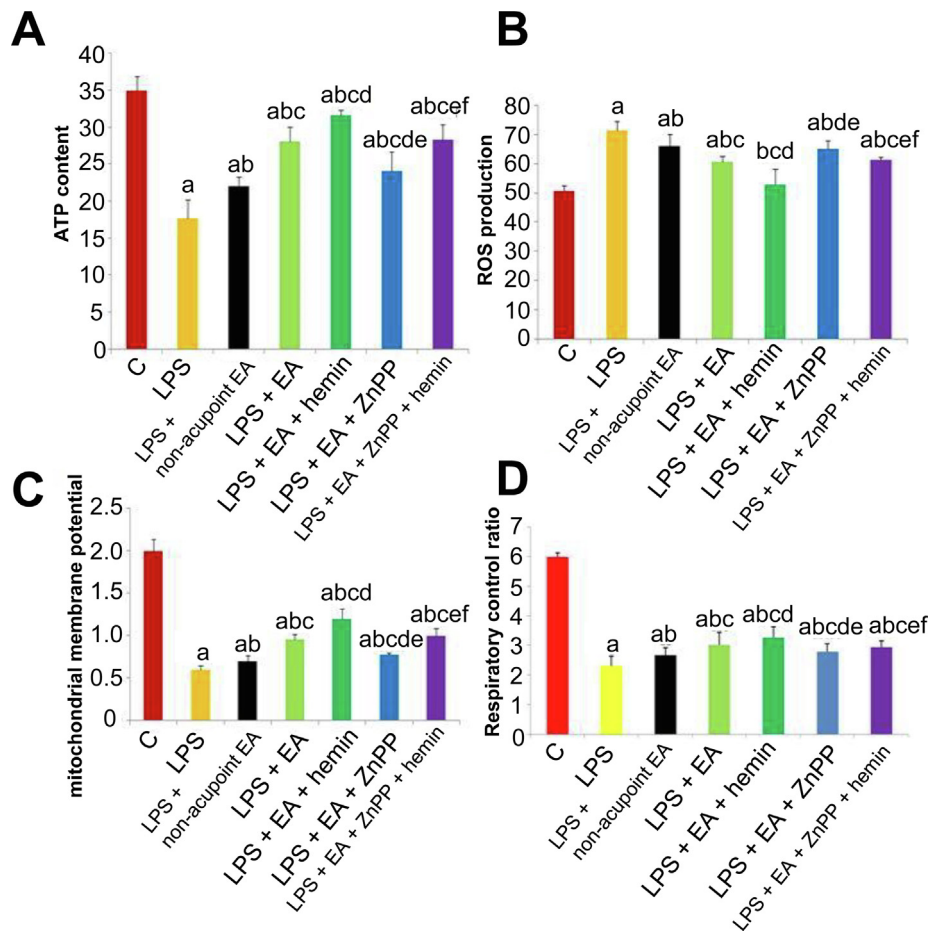


**Fig. 3.** Electroacupuncture and HO-1 upregulation protect against LPS-induced mitochondrial dysfunction. (AD) ATP content (A), ROS production (B), mitochondrial membrane potential (C), and respiratory control ratio (D). Values are expressed as mean  $\pm$  SD ( $n = 10$ ).  $ap < 0.05$  vs. Control group;  $bp < 0.05$  vs. LPS group;  $cp < 0.05$  vs. LPS + non-acupoint EA group;  $dp < 0.05$  vs. LPS + EA group;  $ep < 0.05$  vs. LPS + EA + hemin group;  $f p < 0.05$  vs. LPS + EA + ZnPP group.

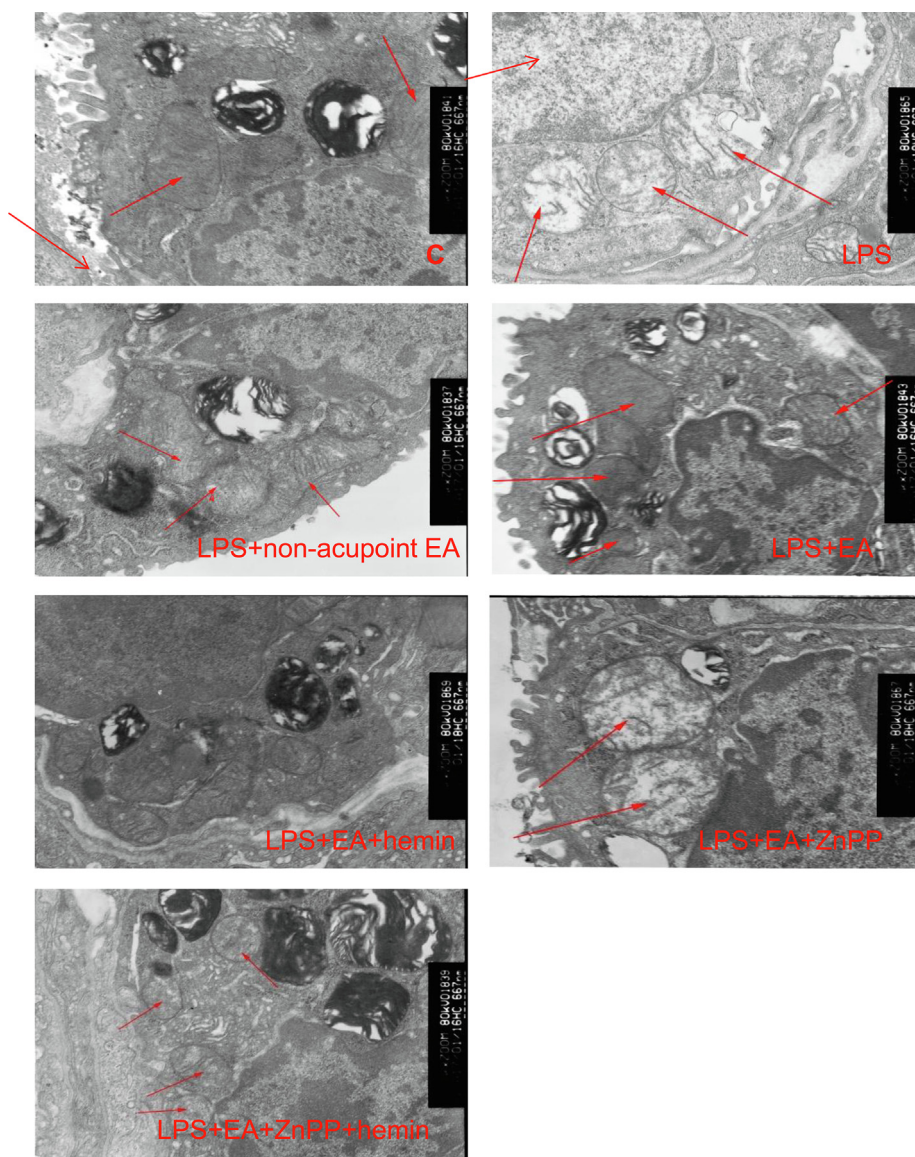


**Fig. 4.** Electroacupuncture and HO-1 upregulation reverse LPS-induced changes in mitochondrial ultrastructure. Electron microscopy images of mitochondria in lung tissues from the C group, LPS + EA group, LPS group, LPS + non-acupoint EA group, LPS + EA + hemin group, LPS + EA + ZnPP group and LPS + EA + ZnPP + hemin group. Red arrows show the mitochondria. 15,000 $\times$  magnification.

strongly suggest that EA improves the LPS-induced ATP reduction, MMP and RCR decrease and ROS increase and mitigates the pathological processes underlying LPS-induced lung injury by augmenting HO-1 expression.

### 3.3. Effects of EA and HO-1 expression on mitochondrial ultrastructure

As shown in Fig. 4, LPS increased mitochondrial edema and crest fracture that were suppressed by EA and further suppressed by hemin, while Znpp-IX injection partially inhibited the protective effects of EA.

### 3.4. Mfn1/2, OPA1, and Drp1 mRNA and protein expression levels

Mfn1/2, as mitochondrial markers, facilitate the mitochondrial location and homotypic fusion (Huang et al., 2017). OPA1, belonging to mitochondria shaping protein family, is also one of mitochondrial markers. As shown in Figs. 5 and 6, LPS injection greatly diminished the expressions of Mfn1, Mfn2, and OPA1 and

enhanced the expression of the mitochondrial fission marker Drp1 at both mRNA and protein levels ( $p < 0.05$ ). Conversely, EA upregulated HO-1, Mfn1, Mfn2, and OPA1 mRNAs and proteins, and downregulated Drp1 mRNA and protein ( $p < 0.05$ ). These changes were significantly enhanced by hemin ( $p < 0.05$ ) and reversed by Znpp-IX ( $p < 0.05$ ).

## 4. Discussion

In this study, we established the paramount importance of HO-1 upregulation in the protective effects of electroacupuncture against LPS-induced acute lung injury. Electroacupuncture successfully mitigated LPS-induced lung injury by preserving mitochondrial function as evidenced by elevating ATP production, maintaining mitochondrial membrane potential, increasing respiratory control ratio and sustaining mitochondrial fusion/fission balance. These protective effects were associated with HO-1 upregulation, and additional HO-1 induction further augmented the protective efficacy of EA; conversely, HO-1 inhibition blocked the

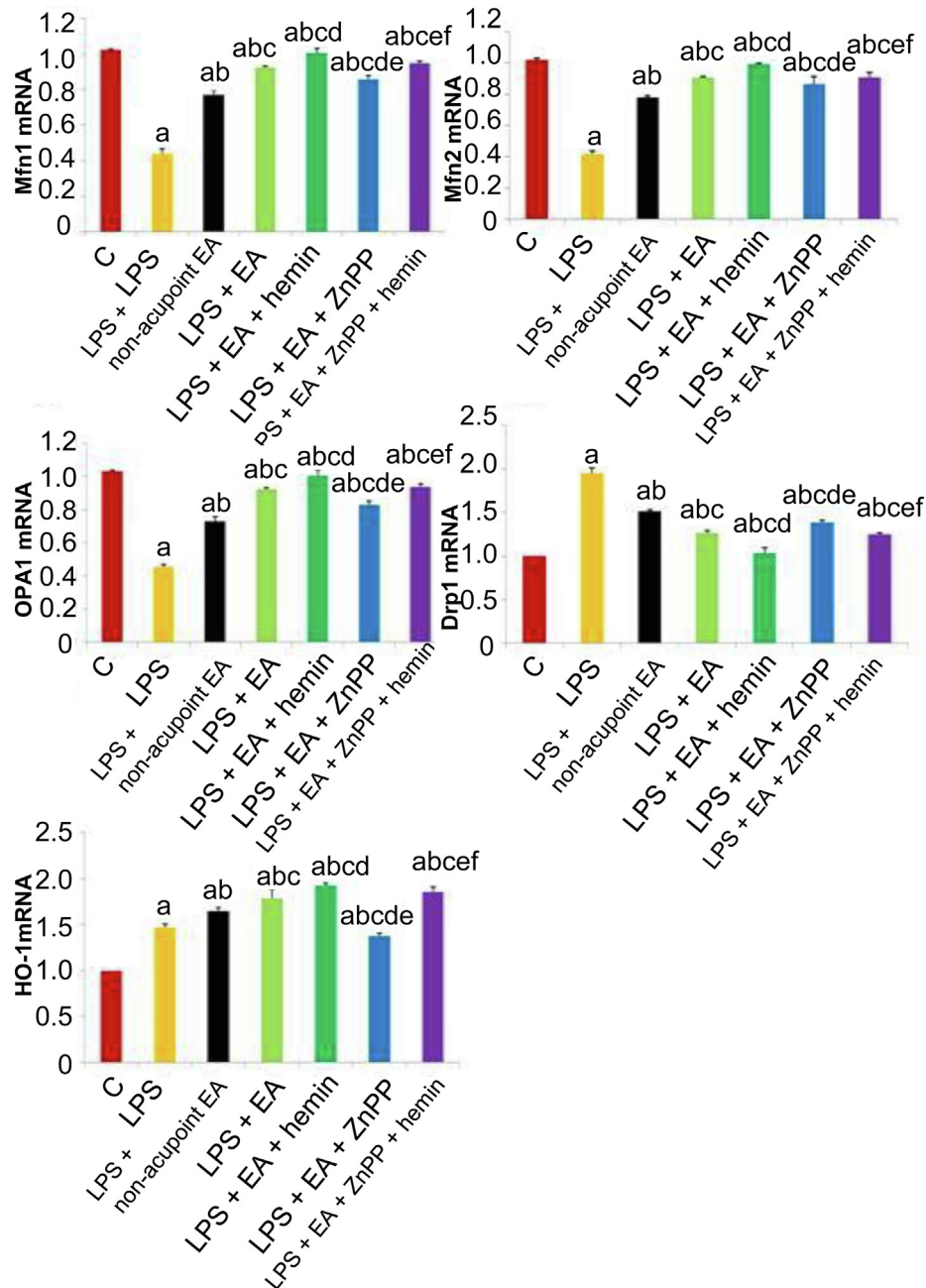


**Fig. 5.** Effects of EA and HO-1 modulators on LPS-induced changes in mitochondrial fusion markers, fission markers, and HO-1 at the mRNA level. Mfn1, Mfn2, OPA1, Drp1, and HO-1 mRNA expression levels in lung tissues were analyzed by RT-PCR. Values are expressed as mean  $\pm$  SD ( $n = 10$ ).  $a_p < 0.05$  vs. Control group;  $b_p < 0.05$  vs. LPS group;  $c_p < 0.05$  vs. LPS + non-acupoint EA group;  $d_p < 0.05$  vs. LPS + EA group;  $e_p < 0.05$  vs. LPS + EA + hemin group;  $f_p < 0.05$  vs. LPS + EA + ZnPP group.

protective effects of EA on LPS-induced lung injury. HO-1 is an inducible stress response protein with demonstrated protective functions in multiple disease states (Araujo et al., 2012; Wegiel et al., 2014), while other studies have reported that EA pretreatment can provide neuroprotection by inhibiting mitochondrial fission (Zhang et al., 2018).

Mitochondrial impairment is a major pathogenic mechanism for organ injury during sepsis (Duvigneau et al., 2008). Excessive ROS generation directly and indirectly disrupts mitochondrial respiratory function (Wen et al., 2014), resulting in mitochondrial membrane depolarization and reduced cellular ATP production (Tatagiba et al., 2017). In this study, we established a sepsis model by LPS treatment. While LPS-induced sepsis models do not recapitulate all clinical features, they can reveal underlying mechanisms, such as oxidative stress and mitochondrial impairment, and poten-

tial treatment strategies. In the current study, LPS induced ALI, fusion/fission imbalance, ROS release, lower ATP production, mitochondrial membrane depolarization, and reduced respiratory control ratio, in accord with our previous studies. Both reduced respiratory control ratio and mitochondrial membrane depolarization in LPS-treated lungs were reversed by EA pretreatment, indicating improved mitochondrial functional status (Solsona-Vilarrasa et al., 2019). Mitochondrial function is also dependent on the balance between fusion and fission, and disruption of this balance is implicated in sepsis-associated organ injury (Gonzalez et al., 2014). Previous studies have demonstrated that LPS triggers oxidative stress-mediated fusion/fission imbalance in lung tissue (Dong et al., 2018), and EA enhanced the expression of fusion markers but reduced the expression of a fission marker, effects augmented by HO-1 induction and reversed by HO-1 inhibition.

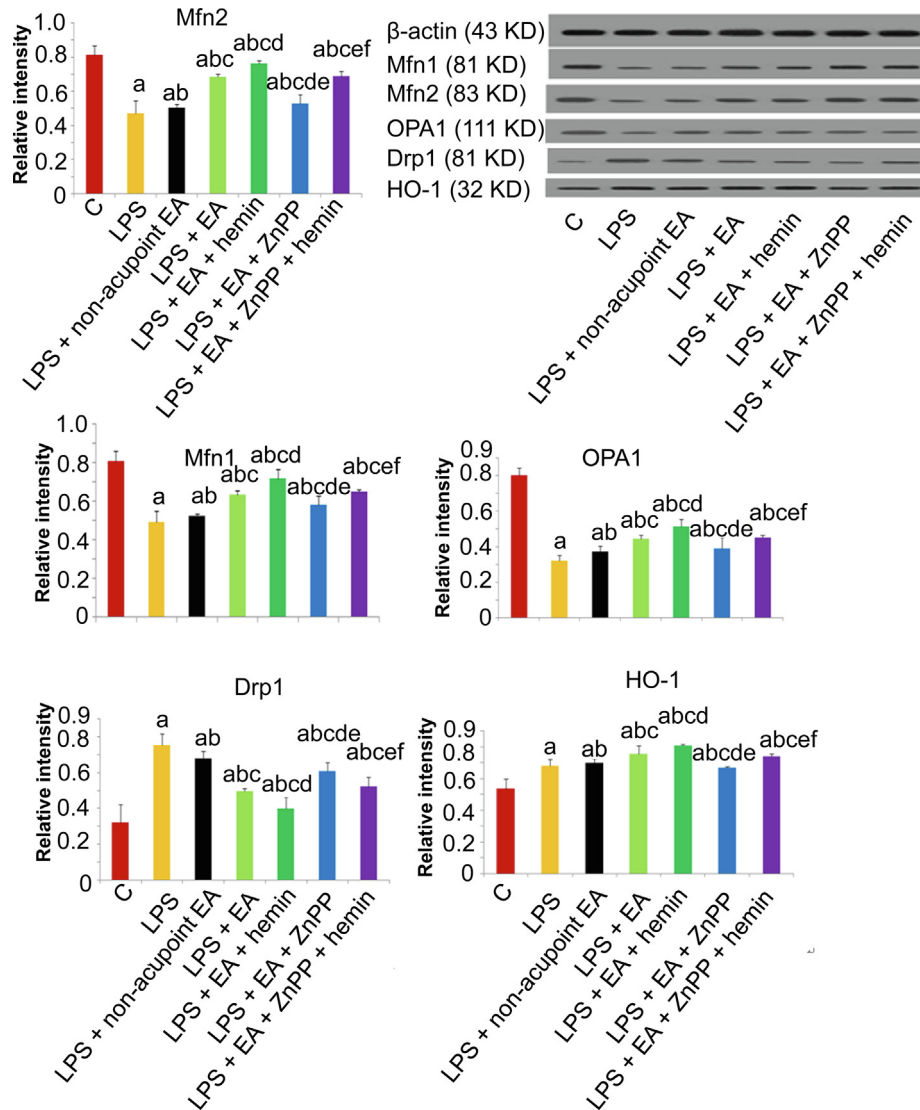


**Fig. 6.** Effects of EA and HO-1 modulators on LPS-induced changes in mitochondrial fusion markers, fission markers, and HO-1 at the protein level. Protein expression levels of Mfn2, Mfn1, OPA1, Drp1 and HO-1 and Values are expressed as mean ± SD (n = 10). ap < 0.05 vs. Control group; bp < 0.05 vs. LPS group; cp < 0.05 vs. LPS + non-acupoint EA group; dp < 0.05 vs. LPS + EA group; ep < 0.05 vs. LPS + EA + hemin group; fp < 0.05 vs. LPS + EA + ZnPP group.

Heme oxygenase-1 is expressed in mitochondria and protects against sepsis-associated organ injury (Slebos et al., 2007). In this study, pretreatment of LPS-treated rabbits with the HO-1 inducer hemin or the HO-1 inhibitor ZnPP-IX was used to ascertain the links among acupuncture, mitochondrial dynamics, and HO-1 expression level. Hemin enhanced the protective effects of EA, upregulated mitochondrial fusion protein expression levels, and downregulated mitochondrial fission protein expression. On the contrary, administration of ZnPP-IX markedly reversed the effects of EA and HO-1 induction, downregulated mitochondrial fusion protein expression, and upregulated mitochondrial fission protein expression. From these results, it appears that regulation of mitochondrial fission and fusion by HO-1 mediates the protective effects of EA against endotoxin-induced ALI.

Numerous studies have shown that stimulation of acupoints is more effective than stimulation of nearby non-acupoint areas (Zhou et al., 2014; Lee et al., 2018). In the current study, EA at acupoints decreased ROS production, increased ATP content, mitochondrial membrane potential, and respiratory control ratio, and sustained the mitochondrial fission/fusion balance through upreg-

ulation of HO-1, while non-acupoint EA only slightly affected mitochondrial dynamics and mitochondrial function.

This study has certain limitations. First, the molecular mechanisms by which HO-1 modulates mitochondrial fusion/fission balance were not examined. Second, although our study demonstrated the selective efficacy of acupoints versus non-acupoints, we did not examine whether EA at ST36 or BL13 acupoints produces more powerful protection. Third, we did not examine whether EA or EA + hemin actually improves survival in this sepsis model.

### 5. Conclusion

In conclusion, this study demonstrates that EA protects against endotoxin-induced ALI by upregulating HO-1. Electroacupuncture successfully mitigated LPS-induced lung injury by preserving mitochondrial function as evidenced by increased ATP content, mitochondrial membrane potential, and respiratory control ratio as well as sustained mitochondrial fusion/fission balance. These findings identify EA and HO-1 modulation as potential strategies against sepsis-induced lung damage.

## Funding statement

This study was supported by the National Natural Science Foundation of China (grant no. 81803899) and the Foundation of Science & Technology Research Project of Tianjin Health Bureau (grant no. 2015KY26).

## Author contributions

Conceptualization, Jian-bo Yu; Methodology, Yuan Zhang and Wei-wei Zhang; Formal Analysis, Jia Shi; Investigation, Tian-yu Yu and Jian-bo Yu; Writing-Original Draft Preparation, Shi-han Du and Si-meng He; Writing-Review and Editing, Kai Song and Jian-bo Yu. Yuan Zhang, Wei-wei Zhang, Jia Shi contributed equally to the manuscript.

## Declaration of Competing Interest

The authors declare that they have no known competing financial interests or personal relationships that could have appeared to influence the work reported in this paper

## References

- Araujo, J.A., Zhang, M., Yin, F., 2012. Heme oxygenase-1, oxidation, inflammation, and atherosclerosis. *Front. Pharmacol.* 3, 119.
- Bueno, M., Lai, Y.C., Romero, Y., Brands, J., Croix, C.M.S., Kamga, C., Corey, C., HerazoMaya, J.D., Sembrat, J., Lee, J.S., Duncan, S.R., Rojas, M., Shiva, S., Chu, C.T., Mora, A.L., 2015. PINK1 deficiency impairs mitochondrial homeostasis and promotes lung fibrosis. *J. Clin. Invest.* 125, 21–38.
- Chen, Y., Lei, Y., Mo, L.Q., Li, J., Wang, M.H., Wei, J.C., Zhou, J., 2016a. Electroacupuncture pretreatment with different waveforms prevents brain injury in rats subjected to cecal ligation and puncture via inhibiting microglial activation, and attenuating inflammation, oxidative stress and apoptosis. *Brain Res. Bull.* 127, 248–259.
- Chen, Z.X., Li, Y., Zhang, X.G., Chen, S., Yang, W.T., Zheng, X.W., Zheng, G.Q., 2017. Sham electroacupuncture methods in randomized controlled trials. *Sci. Rep.* 7, 1–19.
- Chen, L., Liu, Y., Lin, Q.M., Xue, L., Wang, W., Xu, J.W., 2016b. Electroacupuncture at Baihui (DU20) acupoint up-regulates mRNA expression of Neuro D molecules in the brains of newborn rats suffering in utero fetal distress. *Neural Regen Res* 11, 604–609.
- Dong, S.A., Zhang, Y., Yu, J.B., Li, X.Y., Gong, L.R., Shi, J., Kang, Y.Y., 2018. Carbon monoxide attenuates lipopolysaccharide-induced lung injury by mitofusin proteins via p38 MAPK pathway. *J. Surg. Res.* 228, 201–210.
- Du, M.H., Luo, H.M., Tian, Y.J., Zhang, L.J., Zhao, Z.K., Lv, Y., Xu, R.J., Hu, S., 2015. Electroacupuncture ST36 prevents postoperative intra-abdominal adhesions formation. *J. Surg. Res.* 195, 89–98.
- Duvigneau, J.C., Piskernik, C., Haindl, S., Kloesch, B., Hartl, R.T., Hüttemann, M., Lee, I., Ebel, T., Moldzio, R., Gemeiner, M., Redl, H., Kozlov, A.V., 2008. A novel endotoxin-induced pathway: upregulation of heme oxygenase 1, accumulation of free iron, and free iron-mediated mitochondrial dysfunction. *Lab. Invest.* 88, 70–77.
- Ferreira, A.S., Lima, J.G., Ferreira, T.P., Lopes, C.M., Meyer, R., 2009. Prophylactic effects of short-term acupuncture on Zusanli (ST36) in Wistar rats with lipopolysaccharide-induced acute lung injury. *Zhong Xi Yi Jie He Xue Bao* 7, 969–975.
- Gonzalez, A.S., Elguero, M.E., Finocchietto, P., Holod, S., Romorini, L., Miriuka, S.G., Peralta, J.G., Poderoso, J.J., Carreras, M.C., 2014. Abnormal mitochondrial fusion/fission balance contributes to the progression of experimental sepsis. *Free Radic. Res.* 48, 769–783.
- Han, Y.G., Qin, X., Zhang, T., Lei, M., Sun, F.Y., Sun, J.J., Yuan, W.F., 2017. Electroacupuncture prevents cognitive impairment induced by lipopolysaccharide via inhibition of oxidative stress and neuroinflammation. *Neurosci. Lett.* 683, 190–195.
- Huang, X., Zhou, X., Hu, X., Joshi, A.S., Guo, X., Zhu, Y., Chen, Q., Prinz, W.A., Hu, J., 2017. Sequences flanking the transmembrane segments facilitate mitochondrial localization and membrane fusion by mitofusin. *Proc. Natl. Acad. Sci. USA* 114, E9863–E9872.
- Hull, T.D., Boddu, R., Guo, L., Tisher, C.C., Traylor, A.M., Patel, B., Joseph, R., Prabhu, S. D., Suliman, H.B., Piantadosi, C.A., Agarwal, A., George, J.F., 2016. Heme oxygenase-1 regulates mitochondrial quality control in the heart. *JCI Insight* 1, e85817.
- Lee, H.Y., Kwon, O.J., Kim, J.E., Kim, M., Kim, A.R., Park, H.J., Cho, J.H., Kim, J.H., Choi, S.M., 2018. Efficacy and safety of acupuncture for functional constipation: a randomised, sham-controlled pilot trial. *BMC Complement Altern. Med.* 18, 186.
- Li, L., Yu, J.B., Mu, R., Dong, S.A., 2017. Clinical effect of electroacupuncture on lung injury patients caused by severe acute pancreatitis. *Evid. Based Complement Alternat. Med.* 2017, 3162851.
- Liu, Z.S., Liu, Y., Xu, H.F., He, L.Y., Chen, Y.L., Fu, L.X., Li, N., Lu, Y.H., Su, T.S., Sun, J.H., Wang, J., Yue, Z.H., Zhang, W., Zhao, J.P., Zhou, Z.Y., Wu, J.N., Zhou, K.H., Ai, Y.K., Zhou, J., Pang, R., Wang, Y., Qin, Z.S., Yan, S.Y., Li, H.J., Luo, L., Liu, B.Y., 2017. Effect of electroacupuncture on urinary leakage among women with stress urinary incontinence A Randomized Clinical Trial. *JAMA* 317, 2493–2501.
- Long, J., He, C.J., Dai, H., Kang, X.G., Zou, J.F., Ye, S.L., Yu, Q., 2019. Effects of transection of cervical sympathetic trunk on cognitive function of traumatic brain injury rats. *Neuropsychiatr. Dis. Treat.* 15, 1121–1131.
- Nurwati, I., Purwanto, B., Mudigdo, A., Saputra, K., Prasetyo, D.H., Muthmainah, M., 2019. Improvement in inflammation and airway remodelling after acupuncture at BL13 and ST36 in a mouse model of chronic asthma. *Acupunct. Med.* 37, 228–236.
- Pan, P., Zhang, X., Qian, H., Shi, W., Wang, J., Bo, Y., Li, W., 2010. Effects of electroacupuncture on endothelium-derived endothelin-1 and endothelial nitric oxide synthase of rats with hypoxia-induced pulmonary hypertension. *Exp. Biol. Med.* (Maywood) 235, 642–648.
- Privitera, M.G., Potenza, M., Bucolo, C., Leggio, G.M., Drago, F., 2007. Hemin, an inducer of heme oxygenase-1, lowers intraocular pressure in rabbits. *J. Ocul. Pharmacol. Ther.* 23, 232–239.
- Qin, G.H., Wang, J.X., Huo, Y.J., Yan, H.X., Jiang, C.C., Zhou, J.X., Wang, X., Sang, N., 2012. Sulfur dioxide inhalation stimulated mitochondrial biogenesis in rat brains. *Toxicology* 300, 67–74.
- Rubinfeld, G.D., Caldwell, E., Peabody, E., Weaver, J., Martin, D.P., Neff, M., Stern, E.J., Hudson, L.D., 2005. Incidence and outcomes of acute lung injury. *N. Engl. J. Med.* 353, 1685–1693.
- Schlosser, K., Taha, M., Deng, Y.P., McIntyre, L.A., Mei, S.H.J., Stewart, D.J., 2018. High circulating angiotensin-2 levels exacerbate pulmonary inflammation but not vascular leak or mortality in endotoxin-induced lung injury in mice. *Thorax* 73, 248–261.
- Shafeeq, H., Lat, I., 2012. Pharmacotherapy for acute respiratory distress syndrome. *Pharmacotherapy* 32, 943–957.
- Slebos, D.J., Rytter, S.W., van der Toorn, M., Liu, F., Guo, F.L., Baty, C.J., Karlsson, J.M., Watkins, S.C., Kim, H.P., Wang, X., Lee, J.S., Postma, D.S., Kauffman, H.F., Choi, A. M.K., 2007. Mitochondrial localization and function of heme oxygenase-1 in cigarette smoke-induced cell death. *Am. J. Respir. Cell Mol. Biol.* 36, 409–417.
- Solsona-Vilarrasa, E., Fucho, R., Torres, S., Nuñez, S., Nuño-Lámbarrri, N., Enrich, C., García-Ruiz, C., Fernández-Checa, J.C., 2019. Cholesterol enrichment in liver mitochondria impairs oxidative phosphorylation and disrupts the assembly of respiratory supercomplexes. *Redox Biol.* 24, 101214.
- Suzuki, M., Muro, S., Fukui, M., Ishizaki, N., Sato, S., Shiota, T., Endo, K., Suzuki, T., Mitsuma, T., Mishima, M., Hirai, T., 2018. Effects of acupuncture on nutritional state of patients with stable chronic obstructive pulmonary disease (COPD): re-analysis of COPD acupuncture trial, a randomized controlled trial. *BMC Complement Altern. Med.* 18, 287.
- Tatagiba, K.W.M., Rui, C., Carolina, A.L.T., 2017. Autophagy is impaired in neutrophils from streptozotocin-induced diabetic rats. *Front. Immunol.* 8, 24.
- Wang, K., Wu, H.X., Wang, G.N., Li, M.M., Zhang, Z.D., Gu, G.Y., 2009. The effects of electroacupuncture on TH1/TH2 cytokine mRNA expression and mitogen activated protein kinase signaling pathways in the splenic T cells of traumatized rats. *Anesth. Analg.* 109, 1666–1673.
- Wegiel, B., Nemeth, Z., Correa-Costa, M., Bulmer, A.C., Otterbein, L.E., 2014. Heme oxygenase-1: a metabolic nuke. *Antioxid. Redox Signal.* 20, 1709–1722.
- Wen, Z.S., Xiang, X.W., Jin, H.X., Guo, X.Y., Liu, L.J., Huang, Y.N., OuYang, X.K., Qua, Y. L., 2014. Protective effect of polysaccharides from *Sargassum horneri* against oxidative stress in RAW264.7 cells. *Int. J. Biol. Macromol.* 68, 98–106.
- Youle, R.J., van der Blik, A.M., 2012. Mitochondrial fission, fusion, and stress. *Science* 337, 1062–1065.
- Yu, J.B., Dong, S.A., Luo, X.Q., Gong, L.R., Zhang, Y., Wang, M., Cao, X.S., Liu, D.Q., 2013. Role of HO-1 in protective effect of electro-acupuncture against endotoxin shock induced acute lung injury in rabbits. *Exp Biol Med* (Maywood) 238, 705–712.
- Yu, J.B., Shi, J., Wang, D., Dong, S.A., Zhang, Y., Wang, M., Gong, L.R., Fu, Q., Liu, D.Q., 2016. Heme oxygenase-1/carbon monoxide-regulated mitochondrial dynamic equilibrium contributes to the attenuation of endotoxin-induced acute lung injury in rats and in lipopolysaccharide-activated macrophages. *Anesthesiology* 125, 1190–1201.
- Zhang, X.W., Chen, J.X., Xue, M., Tang, Y.Y., Xu, J.Y., Liu, L., Huang, Y.Z., Yang, Y., Qiu, H.B., Guo, F.M., 2019b. Overexpressing p130/E2F4 in mesenchymal stem cells facilitates the repair of injured alveolar epithelial cells in LPS-induced ARDS mice. *Stem Cell Res. Ther.* 10, 74.
- Zhang, J.R., Lin, Q., Liang, F.Q., Xie, T., 2019a. Dexmedetomidine attenuates lung injury by promoting mitochondrial fission and oxygen consumption. *Med. Sci. Monit.* 25, 1848–1856.
- Zhang, G.F., Yang, P., Yin, Z., Chen, H.L., Ma, F.G., Wang, B., Sun, L.X., Bi, Y.L., Shi, F., Wang, M.S., 2018. Electroacupuncture preconditioning protects against focal cerebral ischemia/reperfusion injury via suppression of dynamin-related protein 1. *Neural Regen. Res.* 13, 86–93.
- Zhang, Y., Yu, J.B., Luo, X.Q., Gong, L.R., Wang, M., Cao, X.S., Dong, S.A., Yan, Y.M., Kwon, Y., He, J., 2014. Effect of ERK1/2 signaling pathway in electroacupuncture mediated up-regulation of heme oxygenase-1 in lungs of rabbits with endotoxin shock. *Med. Sci. Monit.* 20, 1452–1460.
- Zhou, Q., Gai, S., Lin, N., Zhang, J., Zhang, L., Yu, R., Liu, J., Cai, X., 2014. Power spectral differences of electrophysiological signals detected at acupuncture points and nonacupuncture points. *Acupunct. Electrother. Res.* 39, 169–181.